Computer Simulation of Flux Pinning in Type-II Superconductors

E. H. Brandt

Institut für Physik, Max-Planck-Institut für Metallforschung, D-7000 Stuttgart 80, West Germany

(Received 28 February 1983)

Random point pinning of ideal or defective flux-line lattices is simulated on a computer. For weak pins, Larkin and Ovchinnikov's two-dimensional collective pinning is confirmed: $j_c = \text{const} \times n_p \langle f_p^2 \rangle / R_p c_{66}$ (j_c is the critical current; n_p, f_p, and R_p are the density, force, and range of pins; and c_{66} is the shear modulus). The constant is determined. Defective lattices are pinned more strongly by factors 1.3 to 3, explaining the observed history effect. A pronounced jump in the curves $j_c(f_p)$ indicates the onset of plastic deformation.

PACS numbers: 74.60.Ge

The statistical summation of pinning forces in type-II superconductors is still a controversial problem. The theory of Labusch,[1] conceived for widely spaced random point pins, appears to disagree with many experiments and to be inconsistent.[2-4] A pinning threshold predicted by this "dilute limit" theory and its improved versions[3] has been reported only once[5] but usually is absent in experiments. Recently, Larkin and Ovchinnikov[6] (LO) proposed a theory of "collective pinning" which was widely believed to underestimate the critical current j_c even more than previous theories. The situation changed very recently when collective pinning, in its two-dimensional (2D) form, was confirmed with high accuracy on sputtered thin films of amorphous Nb_3Ge and Nb_3Si with extremely weak pinning by Kes and Tsuei.[7] The agreement of experiments with the 3D LO theory improved considerably when Thuneberg, Kukijärvi and Rainer[8] showed that the correct microscopic treatment yields elementary pinning forces f_p which are larger than assumed so far.

In this Letter I report on 2D computer simulations of flux pinning which give the following answers to long-standing questions: (a) The 2D LO result, $j_c \sim f_p^2$, is confirmed for weak, and in some cases for arbitrarily strong, pinning. (b) Some functions $j_c(f_p)$ exhibit a pronounced jump but not a genuine threshold. (c) The history effect[8] is due to much stronger pinning of a defective ("amorphous") flux-line lattice (FLL) as compared to the ideal FLL. (d) The observed steep initial slope of the force-displacement curves[9] is reproduced. (e) For strong pinning the existence of a (modified) direct summation limit, $j_c \sim f_p$, is confirmed. (f) The concept of elementary pinning forces should be modified: In order to have simple laws $j_c \propto f_p^2$ and $j_c \propto f_p$ in a large range of pinning strengths, one has to interpret f_p as the root-mean-square pinning force rather than (as is usually assumed) the maximum force, $f_{\max} \approx A_p/R_p$, exerted by a pin with interaction range R_p and amplitude A_p. Depending on the type of pins, relaxation may reduce or enhance f_p from its rigid-lattice value. Typical curves $j_c(f_{\max})$ for attracitve pins exhibit a quadratic region (weak, collective pinning), a jump (onset of plastic FLL deformation), a flat region (flux-line trapping), and a linear, very strong-pinning region.

These results are expected to apply *qualitatively* also to 3D pinning, apart from the weak-pinning law for which a 3D simulation should yield[6,10,11] $j_c \propto f_p^4$. As noticed first by Kes,[12] the LO theory predicts a change of dimensionality, 3D → 2D, when pinning in a film or ribbon (perpendicular to an applied magnetic field) becomes sufficiently weak for the correlation length along the field, L_c, to exceed the film thickness d. In this case our 2D simulation becomes *quantitative* and may help to identify the pins in a given material.

Our simulation starts from the total energy per unit length

$$U = \sum_i \sum_{j \neq i} V_v(|\vec{\mathbf{r}}_i - \vec{\mathbf{r}}_j|) + \sum_i \sum_j V_p(|\vec{\mathbf{r}}_i - \vec{\mathbf{r}}_j^{(p)}|) \tag{1}$$

of a system of N_v vortices with variable positions $\vec{\mathbf{r}}_i = (x_i; y_i)$ and N_p pins with fixed random positions $\vec{\mathbf{r}}_i^{(p)}$ in a roughly quadratic basic area $A = L_x L_y$ with periodic boundary positions. Instead of using the correct interaction potentials between vortices,[13,14] $V_v(r)$, and between vortices and point pins,[15] $V_p(r)$, for better transparency we choose Gaussian-like potentials,

$$V_v(r) = A_v v(r/R_v), \quad V_p(r) = A_p v(r/R_p), \quad v(\rho) \approx \exp(-\rho^2). \tag{2}$$

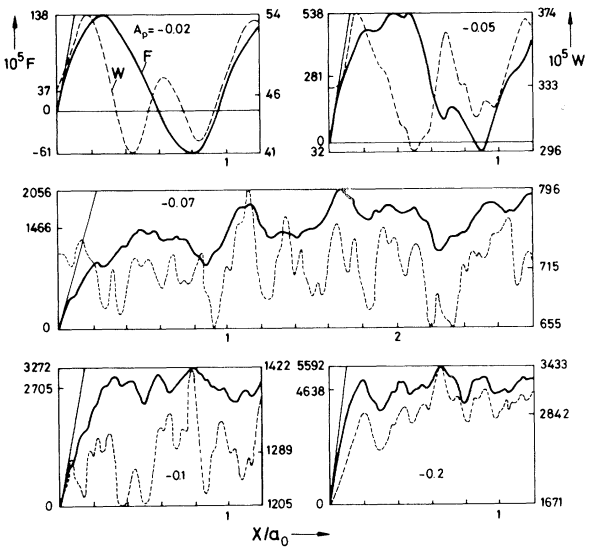

FIG. 1. Mean pinning force $F(X)$ (solid line) and mean square pinning force $W(X)$ (dashed line) vs mean X coordinate of the vortices for $N_v = 780$, $N_p = 210$, $R_v = 0.6$, $R_p = 0.25$, and pin amplitude $A_p = -0.02$, -0.05, -0.07, -0.1, and -0.2 (attractive pins). The numbers on the left (right) denote the maximum and minimum of F (W) in the plotted interval, and the averages $\bar{F}$ ($\bar{W}$) over a much larger interval. Straight lines indicate $F = 0$ and the initial slope of $F(X)$.

We fix our energy and length scales by putting $A_v = 1$ and $a_0 = 1$ (the flux-line spacing). The system is then characterized by five essential parameters: N_v, N_p, R_v, R_p, and A_p. The vortex range $R_v = 0.6$ (0.7, 0.75) determines the shear and compression moduli of the FLL, $c_{66} = 0.2695$ (0.1411, 0.0831) and $c_{11} = 1.994$ (2.345, 2.523) $\gg c_{66}$. Physically, R_v, R_p, and A_p are related to the reduced induction $b = B/B_{c2}$ and to the Ginsburg-Landau parameter κ. For example, $c_{66}/c_{11} \approx (1-b)^2/10b\kappa^2$ ($\kappa^2 \gg 1$, $b \gg 1/2\kappa^2$), for vortex-core pinning $R_p \approx 0.53 b^{1/2}$; and near $b = 1$ we find $A_p = \text{const} \times (1-b)$ and $A_p/c_{66} = \text{const}/(1-b)$ (our main parameter).

At least 72 qualitatively different cases may be distinguished: The pins may be dilute, matching, or dense ($N_p/N_v \ll 1$, ≈ 1, or $\gg 1$), sharp or smooth ($R_p < 0.3$ or > 0.3), repulsive or attractive ($A_p > 0$ or < 0), and strong or weak ($A_p/c_{66}R_p > 1$ or < 1); the initial vortex positions may be ideal triangular FLL with two possible orientations, or amorphous (generated by relaxing random positions). From ≈ 900 cases investigated so far, I present in Figs. 1 and 2 the results of forty runs with $N_v = 780$, $N_p = 210$, $R_v = 0.6$, and $R_p = 0.25$ (attractive and repulsive point pins of

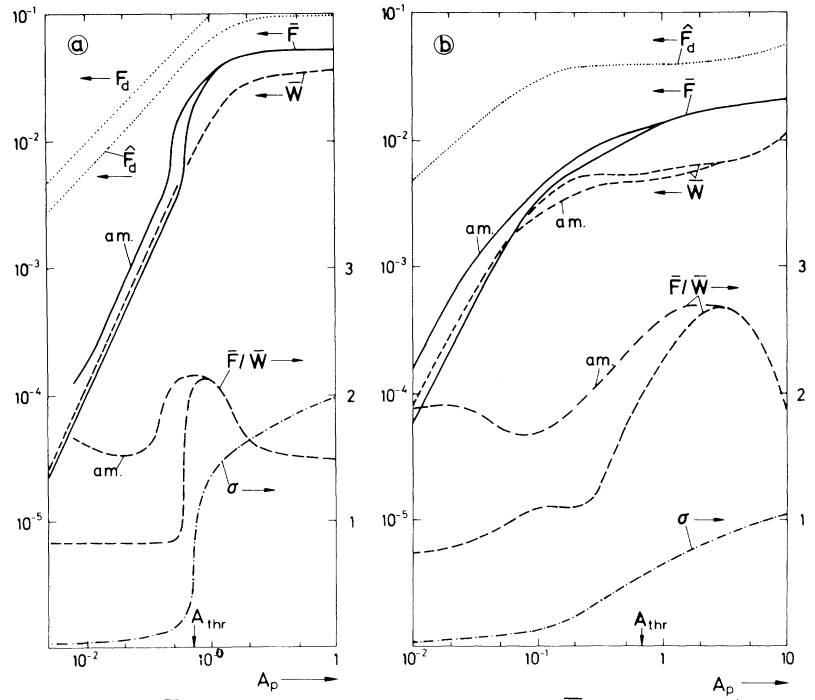

FIG. 2. The averages over X, $\bar{F}$ (solid line, interpreted as j_c) and $\bar{W}$ (short dashes), the direct-summation limits F_d and $\hat{F}_d$, Eq. (4) (dotted lines) (left scale), and the ratio $\bar{F}/\bar{W}$ (long dashes) and the root-mean-square vortex displacement at $X = 1.2$, σ (dash-dotted line) (right scale), plotted vs the pin amplitude A_p. The curves $\bar{F}$ and $\bar{W}$ denoted by "am." are for the amorphous lattice; all other curves are for the ideal lattice or independent of the lattice perfection. The parameters N_v, N_p, R_v, and R_p are as in Fig. 1; (a) attractive pins, (b) repulsive pins.

medium density).

Pinning is simulated in the following way: First the pins are switched on and the FLL is relaxed by minimizing (1). Starting from this virgin state, with $\langle \vec{r}_i \rangle = 0$ by definition, the FLL is shifted homogeneously a small distance $dX \approx 0.001-0.0001$ along $\hat{\vec{x}}$; then the total pinning force is compensated by a homogeneous driving force F acting along $\hat{\vec{x}}$ on each flux line, and the FLL is relaxed by minimizing the function $G = U - N_v F X$ where $X = \langle x_i \rangle$ is the mean x coordinate of the flux lines. By repeating this procedure we should obtain static (i.e., fully relaxed) force-displacement curves $F(X)$ (Fig. 1).[16,17] For weak pinning, $F(X)$ is smooth and periodic, with period a_0 for $\hat{\vec{x}} \parallel \langle 10 \rangle$ and $3^{1/2}a_0$ for $\hat{\vec{x}} \parallel \langle 11 \rangle$. Transient effects slightly "compress" the first periods of $F(X)$. For stronger pinning, $F(X)$ increases first linearly and then fluctuates about its average value $\overline{F}$. If X is oscillated we obtain hysteresis curves oscillating between $+\overline{F}$ and $-\overline{F}$. For comparison with summation theories we calculate also the mean square pinning force $W(X)$ and its average $\overline{W}$. Since the fluctuations of $F(X)$ and $W(X)$ decrease with increasing N_v and N_p, we may relate $\overline{F}$ and $\overline{W}$ to j_c and to the quantity $W(0)$ (Refs. 6 and 7) of large specimens:

$$j_c B = n\overline{F} = n_p \langle\langle -\hat{\vec{x}} \cdot \vec{f}_j(X) \rangle\rangle, \qquad W(0)/d = n\overline{W} = n_p \langle\langle |\vec{f}_j(X)|^2 \rangle\rangle, \tag{3}$$

where $n = N_v/A = B/\varphi_0 = \frac{2}{3}^{1/2} a_0^{-2}$ and $n_p = N_p/A$ are the densities of vortices and pins, $\vec{f}_j = \partial U/\partial \vec{r}_j^{(p)}$ is the force exerted by the ith pin, and the averages are over j and X.

Figure 2 shows $\overline{F}(A_p)$, $\overline{W}(A_p)$, $\overline{F}/\overline{W}$, and the direct summation limit in its old (F_d) and improved[14] ($\hat{F}_d$) versions,

$$F_d \equiv n_p f_{\max}/n = (2/e)^{1/2} N_p A_p / N_v R_p, \qquad \hat{F}_d \equiv n_p f_p / n = (N_p \overline{W}/N_v)^{1/2}. \tag{4}$$

Note that the limit $\hat{F}_d$ is almost reached: $\overline{F} \leq 0.54\hat{F}_d$ for attractive pins, and $\overline{F} \leq 0.42\hat{F}_d$ for repulsive pins. The limit F_d is much too high, and for repulsive pins even makes no sense. For repulsive pins $\overline{W}$ is always below its rigid-lattice (weak pinning) limit,[14] $\pi n_p A_p^2$, whereas for attractive pins the ratio $\overline{W}/\pi n_p A_p^2$ exceeds unity, goes through a flat maximum [≈ 1.3 at $A_p \approx -0.07$ in Fig. 2(a)], and then drops below unity [at $A_p = -0.135$ in Fig. 2(a)].

The perhaps most striking feature is a pronounced *jump* of $F(A_p)$ occurring in Fig. 2(a) almost exactly at the *threshold* value $A_p = -0.071$ predicted from the onset of elastic instabilities for the isolated pin.[1,3,5] For short-range ($R_p < 0.3$) attractive Gaussian pin potential (2) this threshold is at[14]

$$A_{\text{thr}} = 2\pi \exp(\tfrac{3}{2}) c_{66} R_p^2 / \ln(N_v). \tag{5}$$

This jump is most clearly seen in the (linearly plotted) functions $\overline{F}/\overline{W}$ and $\sigma \equiv \langle |\vec{s} - \langle \vec{s} \rangle|^2 \rangle^{1/2}$ (the root-mean-square vortex displacement at $X = 1.2$). The increase of σ indicates the onset of plastic FLL deformation, a conjecture which is confirmed by plots of the vortex and pin positions. Note also the "slowing down" of the fluctuations of $F(X)$ at $A_p = 0.07$ in Fig. 1. The character of $F(X)$ changes just at the jump of $\overline{F}$, again indicating the transition from the "elastic" to the "plastic" range. A similar jump in $\overline{F}/\overline{W}$ occurs for repulsive pins in Fig. 2(b). The transition is broader and starts at a value $A_p \approx 0.3$ which is somewhat smaller than the threshold for repulsive pins,[14] $A_{\text{thr}} \approx 0.7$ in this case. If we start with an amorphous FLL the jump is absent or of smaller amplitude, indicating that our amorphous FLL cannot become much more defective.

For weak pinning the 2D LO result $\overline{F}/\overline{W} = \text{const}$ is confirmed both for the ideal and for the amorphous FLL. For the ideal FLL we obtain

$$\overline{F}/\overline{W} = 0.035[\ln(N_v/33)]^{1/2} R_p c_{66}. \tag{6}$$

The dependence on R_p and c_{66} is well established for $0.6 \leq R_v \leq 0.75$ and $0.0625 \leq R_p \leq 0.4$. For $R_v < 0.6$ or $R_p > 0.4$ compression of the FLL may not be neglected and $\overline{F}/\overline{W}$ depends on c_{66} and c_{11}. Note that for sharp point pins ($R_p \ll 1$) the effective force range is *not* half the vortex spacing [i.e., R_p replaced by $\frac{1}{2}$ in (6)] as is sometimes assumed. For very weak point pins, $\overline{W} = \pi n_p A_p^2$ is independent of R_p but

$$\overline{F} \approx 0.11[\ln(N_v/33)]^{1/2} n_p A_p^2 / R_p c_{66}$$

depends on R_p. The logarithmic factor $\ln(N_v/33) \approx \ln(L_x L_y / 9a_0^2)$ is approximate (for $0.005 \leq A_p \leq 0.05$) and according to the LO theory[6,7] should slightly depend on A_p.

From (3) and (6) we get the 2D collective pinning formula

$$j_c B = W(0)[\ln(R/3a_0)]^{1/2}/20 R_p d c_{66} \tag{7}$$

which, in contrast to LO's estimate, contains a numerically determined prefactor (d and $2R$ are the specimen thickness and width). Equations (6) and (7) apply also to the amorphous FLL if the right-hand sides are multiplied by a factor 1.3

to 3. The enhancement of pinning by the presence of FLL defects usually is considerably larger than the effect of a reduction of c_{66}, which from 3D simulations of amorphous metals is expected to be of the order of 30%. Since defect-enhanced pinning causes the history effect[8] and presumably also the peak in $j_c(B)$ observed near $b=1$ in Ref. 7, the detailed investigation of its mechanism appears to me one of the challenging problems which computer simulations should be able to solve in the near future.

[1]R. Labusch, Cryst. Lattice Defects 1, 1 (1969).
[2]E. J. Kramer, J. Appl. Phys. 49, 742 (1978).
[3]A. M. Campbell, Philos. Mag. B 37, 149 (1978).
[4]E. H. Brandt, Phys. Lett. 77A, 484 (1980).
[5]H. R. Kerchner, J. Narayan, D. K. Christen, and S. T. Sekula, Phys. Rev. Lett. 44, 1146 (1980).
[6]A. I. Larkin and Yu. N. Ovchinnikov, J. Low Temp. Phys. 34, 409 (1979), and references cited therein.
[7]P. H. Kes and C. C. Tsuei, Phys. Rev. Lett. 47, 1930 (1981).
[8]H. Küpfer and W. Gey, Philos. Mag. 36, 859 (1977).
[9]Ch. Rossel, thesis No. 2019, Université de Genève, 1981 (unpublished).
[10]H. R. Kerchner, J. Low Temp. Phys. 46, 205 (1982), and 50, 335 (1983).
[11]D. S. Fisher, "Threshold Behavior of Charge Density Waves Pinned by Impurities" (to be published).
[12]P. H. Kes, private communication.
[13]E. H. Brandt, J. Low Temp. Phys. 28, 263, 291 (1977).
[14]E. H. Brandt, to be published.
[15]E. V. Thuneberg, J. Kukijärvi, and D. Rainer, Phys. Rev. Lett. 48, 1853 (1982).
[16]Dynamic force-velocity curves (interpreted as current-voltage curves) will be given elsewhere.
[17]For one-dimensional simulations see J. R. Appleyard, J. E. Evetts, and A. M. Campbell, Solid State Commun. 14, 567 (1974).